Efficient Sampling for Grasp Quality Evaluation on Gaussian Process Implicit Surface Representations [v-12 09-30-2014]

Michael Laskey, Zoe McCarthy, Jeff Mahler, Florian T. Pokorny, Sachin Patil,
Danica Kragic, Pieter Abbeel, and Ken Goldberg

Abstract—**Gaussian Process Implicit Surface (GPIS) have emerged recently as a new Bayesian shape representation. Former methods for grasp evaluation with shape uncertainty require sampling from distributions on shape. The standard approach of drawing samples from a GPIS in 2D by means of a evaluation on a uniform grid has a complexity of $O(n^6)$(2D) and $O(n^9)$ in the number of grid steps n.We propose an alternative approximationto sampling from shape distributions and demonstrate how that reduce complexity from $O(n^6)$ in 2D and $O(n^9)$ in 3D to $O(n^3)$ for evaluation of a single grasp. We furthermore introduce the idea of adaptive sampling in this context by formulating it as a multi-arm bandit problem for speeding up the selection of the highest quality grasp in a set of proposed grasps.**

I. INTRODUCTION

[TODO: GET HIGH RES GPIS VISUALIZATIONS, INCORPORATE NEXT ROUND OF FEEDBACK] Consider a robot packing boxes in a shipping warehouse environment. The robot will frequently encounter objects that it has not seen before. The robot will have to plan stable grasps without any prior information other than its sensor data. As seen in Fig. 1, with today's RGB and depth sensors, surface properties, such as specularity and transparency, can greatly effect the returned observations. Grasp planners based on deterministic algorithms are not designed to handle such noise and could fail. To plan grasps in a partially observed world, recent research has focused on incorporating uncertainityin the shape of the object [1], [2], [3].

While past work has encoded uncertainty in a polygonal mesh representation [1], an alternative is to work with the signed distance fields (SDFs), a continuous real-valued function that is an implicit surface: zero-valued at the surface of the object, positive value outside the surface and negative valued inside the surface. This representation is growing in popularity in the robotics field for its ability to integrate range data in real time [4], [5]. To incorporate uncertainty one can use a Gaussian Process Implicit Surface (GPIS), a Gaussian process over signed distance field. Not only does GPIS present a straightforward and formal way to incorporate measurements from visual, laser and tactile sensors, they also allow for a differentiable function as a shape representation, which can be used for a feedback grasp controller, finding locally optimal grasps and active exploration [6], [?], [7].

Given a method to represent shape uncertainty, a common technique to evaluate grasp quality is to sample from the distribution on shape and perform Monte-Carlo integration on a given grasp metric [1], [8], [2]. Applying this technique to
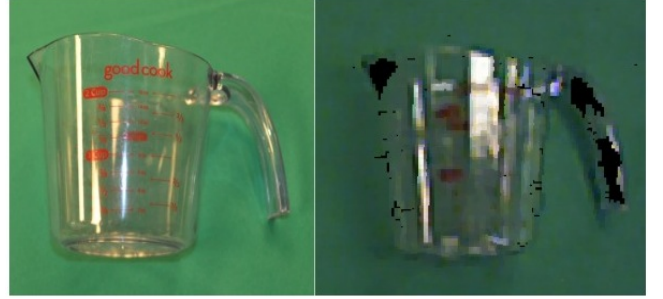

Fig. 1: Left: HD image of a common measuring cup from in a household environment. Right: Image taken from PR2's Primesense Carmine sensor, large parts of the measuring cup are not detected by the depth sensor and are not visible in the RGB image.

GPIS requires an exhaustive sampling of the signed distance field, which scales $O(n^6)$ for a 2D $n \times n$ workspace and $O(n^9)$ for a 3D workspace.The computationally complexity of sampling is derived from the fact sampling from a Gaussian requires matrix inversion of the entire signed distance field. Our paper reduces this complexity to $O(n^3)$ by using the insight that for grasp quality evaluation one only cares about the parameters that define a grasp: contacts points, surface normals, center of mass and friction coefficient [9]. We constrain the contact points by considering the approach trajectory of a gripper. Hence, sampling the whole signed distance field is not needed, but instead one can only work with the distributions on grasp parameters given the shape uncertainty model and gripper trajectory. In light of this our contributions are the following:

1) Derivation of distributions on grasp parameters given GPIS shape uncertainty model and approach trajectory of gripper.
2) Demonstrating both theoretically and empirically how those distributions reduce the computational complexity of sampling.
3) Applying adaptive sampling techniques to efficiently find high quality grasps in a given set of proposed grasps.

II. RELATED WORK

Past work on grasping under uncertainty has focused on state uncertainty [10], [?], [11], uncertainty in object pose [2], [12], [?] or uncertainty in the location of contact with the object [3]. Robust grasp selection for parallel jaw grippers on uncertain shapes was studied by Kehoe et al. for both

zero-slip push grasps [8] and slip push grasps [1] using Monte Carlo integration for the expected grasp quality, but this approach was limited to polygonal shapes. Christopoulo et al. sampled spline fits for 2-dimensional planar objects to measure the quality of uncertainty, however it is has not been shown how a spline based method could incorporate non-visual sensing information for representing shape uncertainty.

The choice of using Gaussian Process Implicit Surfaces to represent uncertainty, is based on the fact it provides a formal way to include various sources of noise from observations such as tactile, laser and visual. Futhermore, implicit surface representations are becoming increasingly popular in robotics due to their success in real-time surface modeling from range images [5], [4], [13]. Some exciting work done with GPIS representation are the following: Hollinger et al. used GPIS to perform active sensing on the hulls in underwater boats [7]. Dragiev et al. showed how GPIS can represent shapes for grasps and used as a grasp controller on the continuous signed distance function [6]. Mahler et al. used GPIS representation to find locally optimal grasps by framing grasp planning as an optimization problem [**?**].

For grasp quality evaluation with shape uncertainty a common method involves sampling from the distribution on shape [1], [8], [2]. With GPIS this requires computationally intensive sampling from a signed distance field that is the dimension of the workspace. We propose an alternative distribution to sample from, based on the idea that we only need to consider the approach trajectory of the gripper.

Monte-Carlo integration involves drawing random samples from a distribution to approximate an integral [14]. While previous work has looked at quality evaluation of a single grasp with uncertainty [2], [3], few have compared many different grasps with uncertainty and efficiently chosen the best one. Adaptive Sampling is the idea of allocating samples based on previous observations or rewards, which can be described as a multi-arm bandit problem [15]. Prior work by Kehoe et al. [8] used an adaptive sampling approach that removed low quality grasps based on values received, but this method had no statistical guarantees and could lead to high quality grasps being removed. To achieve guarantees, we frame the problem as a "budgeted multi-arm bandit" problem, where exploration and exploitation are decoupled and the agent has to allocate resources to explore for a finite time then decide which arm to exploit [16]. Drawing from the literature on Monte-Carlo sampling we estimate the confidence bounds of grasps and prune only those that are statistically distinguishable [14].

III. PRELIMINARIES AND PROBLEM STATEMENT

In this section we describe the mathematical derivation of Gaussian Process Implicit Surface representations.

A. Gaussian Process (GP) Background

GPs provide an infinite dimensional analogue of Multivariate Gaussian Distributions which allow us to model distributions over functions. Gaussian processes (GPs) are widely used in machine learning as a nonparametric regression method for estimating continuous functions from sparse and noisy data [17]. In a GP, a training set consists of input vectors $\mathcal{X} = \{\mathbf{x}_1, \ldots, \mathbf{x}_n\}$, $\mathbf{x}_i \in \mathbb{R}^d$, and corresponding observations $\mathbf{y} = \{y_1, \ldots, y_n\}$. The observations are assumed to be noisy measurements from the unknown target function f:

$$y_i = f(\mathbf{x}_i) + \epsilon, \tag{1}$$

where $\epsilon \sim \mathcal{N}(0, \sigma^2)$ is Gaussian noise in the observations. A zero-mean Gaussian process is completely specified by a covariance function $k(\cdot, \cdot)$, also referred to as a kernel. Given the training data $\mathcal{D} = \{\mathcal{X}, \mathbf{y}\}$ and covariance function $k(\cdot, \cdot)$, the posterior density $p(f_*|\mathbf{x}_*, \mathcal{D})$ at a test point $\mathbf{x}_*$ is shown to be [17]:

$$p(f_*|\mathbf{x}_*, \mathcal{D}) \sim \mathcal{N}\big(\mu(\mathbf{x}_*), \Sigma(\mathbf{x}_*)\big)$$
$$\mu(\mathbf{x}_*) = k(\mathcal{X}, \mathbf{x}_*)^\intercal (K + \sigma^2 I)^{-1} \mathbf{y}$$
$$\Sigma(\mathbf{x}_*) = k(\mathbf{x}_*, \mathbf{x}_*) - k(\mathcal{X}, \mathbf{x}_*)^\intercal (K + \sigma^2 I)^{-1} k(\mathcal{X}, \mathbf{x}_*))$$

where $K \in \mathbb{R}^{n \times n}$ is a matrix with entries $K_{ij} = k(\mathbf{x}_i, \mathbf{x}_j)$ and $k(\mathcal{X}, \mathbf{x}_*) = [k(\mathbf{x}_1, \mathbf{x}_*), \ldots, k(\mathbf{x}_n, \mathbf{x}_*)]^\intercal$. This derivation can also be used to predict the mean and variance of the function gradient by extending the kernel matrices using the identities [18]:

$$\mathrm{cov}\,(f(\mathbf{x}_i), f(\mathbf{x}_j)) = k(\mathbf{x}_i, \mathbf{x}_j) \tag{2}$$
$$\mathrm{cov}\left(\frac{\partial f(\mathbf{x}_i)}{\partial x_k}, f(\mathbf{x}_j)\right) = \frac{\partial}{\partial x_k} k(\mathbf{x}_i, \mathbf{x}_j) \tag{3}$$
$$\mathrm{cov}\left(\frac{\partial f(\mathbf{x}_i)}{\partial x_k}, \frac{\partial f(\mathbf{x}_j)}{\partial x_l}\right) = \frac{\partial^2}{\partial x_k \partial x_l} k(\mathbf{x}_i, \mathbf{x}_j) \tag{4}$$

For our kernel choice we decided to use the square exponential kernel, a major reason for this was its differentiability. Other kernels relevant to GPIS are the thin-plate splines kernel and the Matern kernel [19].

We construct a GPIS by learning a Gaussian Process to fit measurements of a signed distance field of an unknown object. Precisely, $x_i \in \mathbb{R}^2$ in 2D and $x_i \in \mathbb{R}^3$ in 3D, and $y_i \in \mathbb{R}$ is a noisy signed distance measurement to the unknown object at x_i.

B. Line of Action

Similar to the work of [2], we assume that each gripper finger approaches along a *line of action*, a 1D curve $\gamma(t)$ with endpoints a and b as seen in Fig. 3. A gripper finger starts at point a and moves towards b, we assume a is far enough away to be collision free of the object. Each gripper contact is defined by a line of action, so we assume the following tuple is provided $\Gamma = (\gamma_1(\cdot), ..., \gamma_m(\cdot))$, which designates a proposed *grasp plan*.

C. Problem Definition

Given a 2-D workspace $\mathcal{W}$, with an unknown object represented as a trained GPIS model and set of possible grasp plans G. We are interested in determining

$$\Gamma^* \in \mathrm{argmax}_{\Gamma \in G} E(Q(\Gamma)) \tag{5}$$

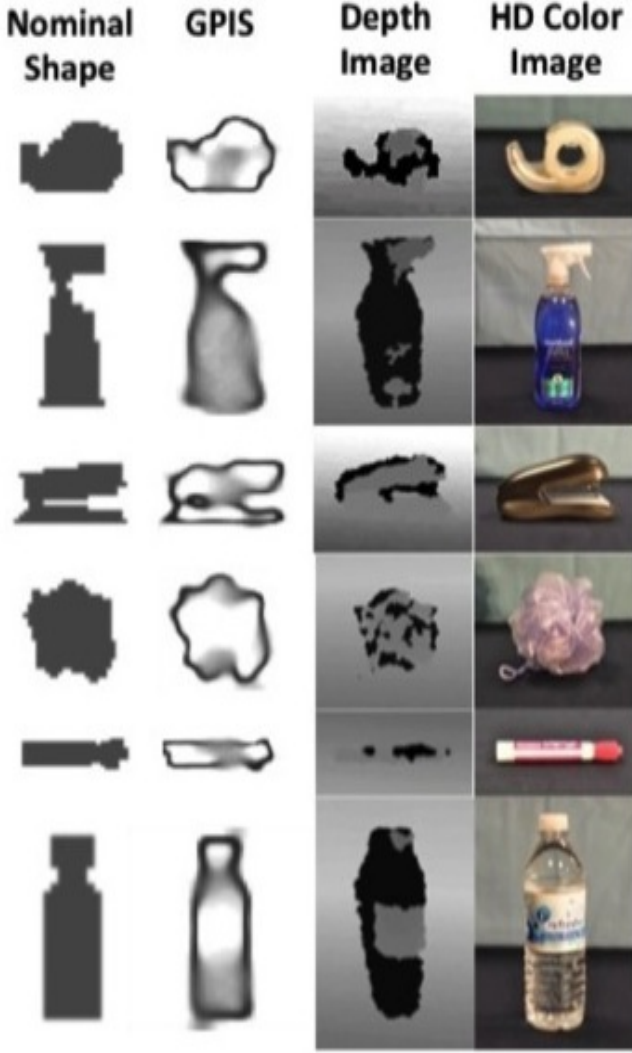with respect to a chosen grasp metric Q.

Fig. 2: Six example objects illustrating transparency, specularity, sensor noise that illustrate the need for shape uncertainty: (from top to bottom) tape, squirt bottle, stapler, loofa, marker, water bottle. Displayed from right to left are the HD color image, a point cloud observation from a Primesense Carmine, GPIS visualization technique from [?], the nominal shape on a 25×25 grid.
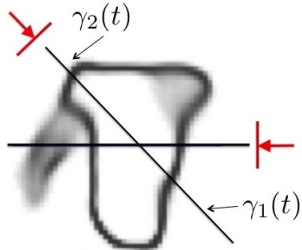

Fig. 3: Illustration of a grasp plan Γ composed of two lines of action, $\gamma_1(t)$ and $\gamma_2(t)$

IV. EVALUATING A GRASP

In order to solve our problem definition, we must evaluate $E(Q(\Gamma))$ for a given grasp plan Γ. We will first discuss which grasp metric Q we chose and then proceed into evaluating the expectation E efficiently.

A. Grasp Metric

In their pioneering work over two decades ago Ferrari and Canny [20], demonstrated a method to rank grasps by considering their contact points and surface normals. Importantly the magnitude of Q yields a measurement that allows one to rank grasps by their physical stability and evaluate the property of force-closure. Furthermore, it has wide spread use in grasp packages like GraspIT[21], OpenGrasp[22] and Simox [23], which motivates studying its effect with uncertainties.

The L^1 version of the metric works by taking as input the contact points $\mathbf{c}_1, ..., \mathbf{c}_m$, surface normals $\mathbf{n}_1, ..., \mathbf{n}_m$, center of mass z and friction coefficient μ. Then constructing a convex hull around the wrenches made up of those parameters and finding the radius of the largest unit ball centered at the origin in wrench space. A wrench is defined as concatenation of a force and torque vector. If the convex hull doesn't enclose the origin, the grasp is not in force-closure. Thus a grasp can be parameterized by the following tuple $g = \{\mathbf{c}_1, ..., \mathbf{c}_m, \mathbf{n}_1, ..., \mathbf{n}_m, \mu, \mathbf{z}\}$, our method is applicable to all grasp metrics that represent a grasp as the tuple g, such as [2], [24].

B. Calculating the Expected Grasp Quality

Given a proposed grasp plan Γ, the expected grasp quality can be evaluated as follows:

$$E(Q(\Gamma)) = \int Q(g|S, \Gamma)p(S)dS \qquad (6)$$

Where $Q(g|S, \Gamma)$ is the grasp quality that is computed on a shape sample drawn from $p(S)$. To compute this we intersect the zero crossing of the level set with the propose grasp plan Γ and determine the parameters g, this has been the approach taken in previous work [1], [8], [2]. See Fig. 4 for an example of what samples drawn from $p(S)$ induced by GPIS look like. For computational reasons we approximate the integral via Monte-Carlo Integration. We use importance sampling to draw from the distribution induced by GPIS and calculate the following
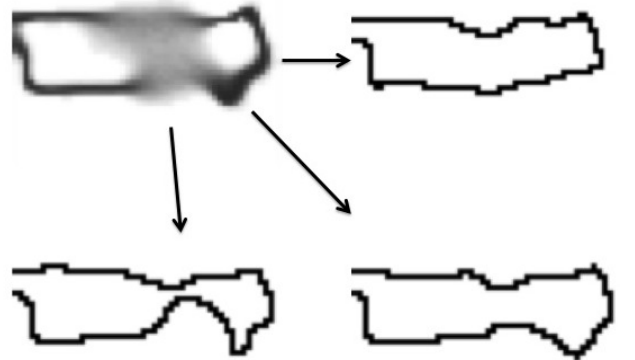

Fig. 4: Shape samples drawn from Eq. 7 on the object in the upper left corner. Given a shape sample we highlight the zero-crossing of the level set in black

$$E(Q(\Gamma)) \approx \sum_{i=1}^{N} Q(g|S_i, \Gamma), S_i \in p(S)$$

To compute the above distribution we must draw samples from $p(S)$. In order to draw shape samples from a GPIS, one needs to sample from signed distance function, sd, over the joint on all points in the workspace $\mathcal{W}$ or $p(sd(\mathcal{W}))$. Since this is a GPIS, we know the following

$$p(S) = p(sd(\mathcal{W})) \sim N(\mu(\mathcal{W}), \Sigma(\mathcal{W})) \qquad (7)$$

Thus if the workspace is an $n \times n$ grid, the joint distribution is an n^2 multi-variate Gaussian, due to $sd : \mathbb{R}^2 \rightarrow \mathbb{R}$. Sampling from a Gaussian involves inverting the covariance matrix and inversion is in the naive way $O(n^3)$ [25]. Thus the complexity of this operation is $O(n^6)$ in 2D and $O(n^9)$ in 3D.

To reduce complexity we propose sampling not from the shape distributions, but instead from the distributions on the grasps parameters themselves. We recall that a grasp according to our metric is defined as the tuple $g = \{\mathbf{c}_1, ..., \mathbf{c}_m, \mathbf{n}_1, ..., \mathbf{n}_m, \mu, z\}$. We are thus interested in calculating $p(g|\Gamma, \mu(x), \Sigma(x))$. The distribution on a grasp is defined then as:

$$p(g) = p\big(\mathbf{c}_1, ..., \mathbf{c}_m, \mathbf{n}_1, ..., \mathbf{n}_m | \Gamma, \mu(x), \Sigma(x)\big) \qquad (8)$$

We note here that we currently use the friction coefficient μ and the expected center of mass $\bar{z}$ as deterministic values. For grippers that do not approach along the same line of action (i.e. non-parallel jaw grippers) we make the assumption that each contact and normal pair is independent, or

$$p(g) = \prod_{i=1}^{m} p\big(\mathbf{c}_i, \mathbf{n}_i | \gamma_i(t), \mu(x), \Sigma(x)\big) \qquad (9)$$

We compute the expected grasp quality now as follows:

$$E(Q(\Gamma)) = \sum_{i=1}^{N} Q(g_i), g_i \in p(g) \qquad (10)$$

We will now show how these distributions can be computed and how the complexity for evaluating a grasp is reduced from $O(n^6)$ to $O(n^3)$.

V. DISTRIBUTION OF GRASP PARAMETERS

To sample from $p(g)$, we need to sample from the distributions associated with a line of action $p(\mathbf{n}_i, \mathbf{c}_i | \gamma_i(t), \mu(x), \Sigma(x))$. Using Bayes rule we can rewrite this as

$$p(\mathbf{n}_i, \mathbf{c}_i | \gamma_i(t), \mu(x), \Sigma(x)) =$$
$$p(\mathbf{n}_i | \mathbf{c}_i, \gamma_i(t), \mu(x), \Sigma(x)) p(c_i | \gamma_i(t), \mu(x), \Sigma(x))$$

In section V-A, we look at how to sample from $p(\mathbf{c}_i | \gamma_i(t), \mu(x), \Sigma(x))$. Then in section V-B, we look at how to sample from $p(\mathbf{n}_i | \mathbf{c}_i, \gamma_i(t), \mu(x), \Sigma(x))$ and present a

novel visualization technique for the distribution on surface normals. Lastly in section V-C, we show a way to calculate the expected center of mass assuming a uniform mass distribution. .

A. Distribution on Contact Points

We would like to find the distribution on contact point $\mathbf{c}_i$. A contact point in terms of the GPIS and line of action model can be defined as the point, t, when the signed distance function is zero and no points before said point along the line have touched the surface. We express this as the following conditions:

$$sd(\gamma(t)) = 0 \qquad (11)$$
$$sd(\gamma(\tau)) > 0, \ \forall \tau \in [a, t) \qquad (12)$$

We will now demonstrate how to efficiently sample from these distributions and then show what this implies formally.

The probability distribution along the line $\gamma(t)$ is given by:

$$p\big(sd(\gamma(t)); \mu(t), \Sigma(t)\big) \ \forall t \in [a, b] \qquad (13)$$

This gives the signed distance function distributions along the entire line of action in the workspace as a multivariate Gaussian. One could think of this as a marginalization of all other points in signed distance field except the line of action. To sample contact points, one can simply draw samples from Eq. 3 and iterate from a to b until they reach a point that satisfies conditions **??**.

We would like to find the distribution on contact point $\mathbf{c}_i$, which we can define as when the signed distance function $sd(\gamma(t))$ is 0 and all previous times τ we have $sd(\gamma(\tau)) > 0$ for all τ such that $0 \leq \tau < t$. We thus compute this as the joint distribution $p\big(\mathbf{c}_i = \gamma(t)\big) = p\big(sd(\gamma(t)) = 0, sd(\gamma(\tau)) > 0\big) \ \forall \tau \in [0, t)$.

We now derive this distribution:

$$p\big(\mathbf{c}_i = \gamma(t)\big) = \qquad (14)$$
$$\frac{1}{\eta} p\big(sd(\gamma(t)) = 0\big) P\big(sd(\gamma(\tau)) > 0 | sd(\gamma(t)) = 0\big) \qquad (15)$$
$$\forall \tau \in [0, t) \qquad (16)$$

Where η is a proportionality constant. The first product in the equation can be computed easily using the marginalization of a multivariate Gaussian distribution and the second term can be solved by first conditioning on the joint $p(sd(\gamma(t))|sd(\gamma(t)) = 0)$ and then computing the cumulative distribution function [25]. We show the theoretical distribution on $\mathbf{c}_i$ calculated for a given GPIS and line of action in Fig. 5.

In practice Eq. 14 is not efficient to compute because it requires computation of the cumulative distribution function of a large multivariate Gaussian, so instead we sample from Eq. 13 and find the first positive to negative zero-crossing of the sample along the line.
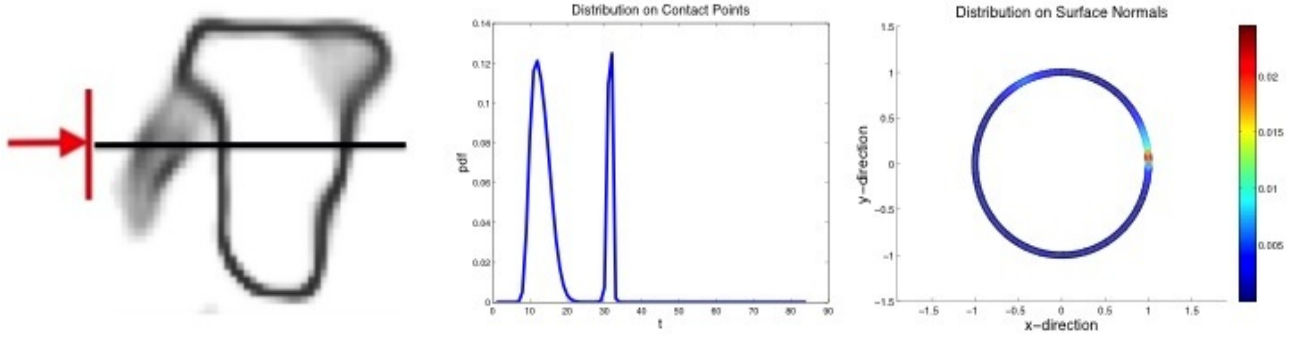
Fig. 5: (Left to Right): Line of action for a given gripper on an uncertain surface representing a measuring cup. Distribution $p(c)$ as a function of t, the position along the line of action $\gamma(t)$. The two modes correspond to the different potential contact points, either the handle or the base of the cup. Lastly, the distribution on the surface normals (inward pointing) along $\gamma(t)$ described by equation **??**.

B. Distribution on Surface Normals

Using Eq. 3 and Eq. 4, we can compute the mean of the gradient $\mu_\nabla(x)$ and the covariance of the gradient $\Sigma_\nabla(x)$ respectively. Thus we can compute the distribution around the surface normal for a given point in $\mathcal{W}$. We can now write

$$p\big(\mathbf{n}_i|\mathbf{c}_i = \gamma(t)\big) = p\big(\mathbf{n}_i|\mu(\gamma(t)), \Sigma(\gamma(t))\big)$$

One interesting effect of this technique is that we can now marginalize out the line of action model and visual what the surface normal distribution is along a given line of action. To our knowledge this is the first attempt to visual surface normals along a grasp plan. Marginalization can be performed as follows:

$$p(\mathbf{n}_i) = \int_a^b p\big(\mathbf{n}_i = \mathbf{v}|\mathbf{c}_i = \gamma(t)\big)p\big(\mathbf{c}_i = \gamma(t)\big)dt \qquad (17)$$

Grasp metrics such as Ferrari-Canny require $\mathbf{n}_i$ be normalized, or, equivalently, a member of the sphere $\mathcal{S}^{d-1}$ [20]. To account for this we densely sample from the distribution $p\big(\mathbf{n}_i)\big)$ and project onto $\mathcal{S}^{d-1}$. In Fig.**??**, we visualize the theoretical distribution on $\mathbf{n}_i$ calculated for a given GPIS and approach line of action.

C. Expected Center of Mass

We recall the quantity $P(sd(x) < 0) = \int_{-\infty}^0 p(sd(x) = s \mid \mu(x), \Sigma(x))ds$ is equal to the probability that x is interior to the surface under the current observations. We assume that the object has uniform mass density and then $P(sd(x) < 0)$ is the expected mass density at x. Then we can find the expected center of mass as:

$$\bar{z} = \frac{\int_\mathcal{W} xP(sd(x) < 0)dx}{\int_\mathcal{W} P(sd(x) < 0)dx} \qquad (18)$$

which can be approximated by sampling $\mathcal{W}$ in a grid and approximating the spatial integral by a sum. Since this operation involves the entire SDF, one would want to use a low resolution grid for computational efficiency. We show the computed density and calculated expected center of mass for a marker in Fig. 6.
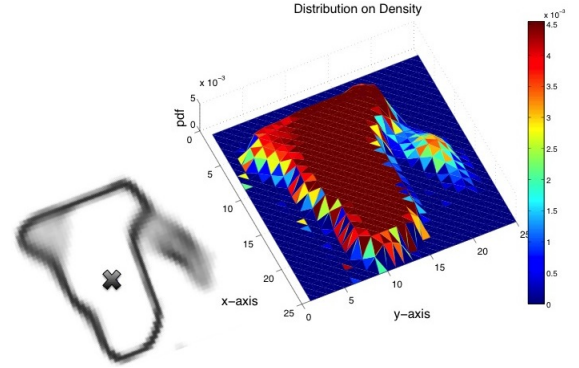

Fig. 6: Left: A surface with GPIS construction and expected center of mass (black X) Right: The distribution on the density of each point assuming uniform density

D. Complexity Analysis on Sampling From Grasps Distributions

After formally deriving each distribution, we can now sample along each line of action $\gamma_i(t)$ from the joint distribution $p(\mathbf{c}_i, \mathbf{n}_i|\gamma_i(t))$, due to our independence assumption Eq. 9. This can be done by drawing samples from Eq. **??**. and using our projection technique for the normal distribution.

Having a distribution along a line of action model allows us to sample from those instead of the joint distribution $p(sd(\mathcal{W}))$. Assuming the line of action is on the order of n, sampling from this distribution for a single grasp is $O(n^3)$. However, each proposed grasp plan Γ requires the distribution to be computed, so if we have $T = |G|$ then the complexity is $O(Tn^3)$. In practice, this should be much smaller than $O(n^6)$.

VI. ADAPTIVE SAMPLING FOR GRASP SELECTION

After determining how to efficiently compute the $E(Q(\Gamma))$, we need to now compute the full problem of Eq. 5, hence the selecting the best grasp plan Γ^*. While a standard approach to solving this problem would be to simply perform Monte-Carlo integration on each Γ_i and compute the expected grasp quality, we propose treating the problem as a multi-arm bandit problem and forming a policy for selecting which grasp to sample. The motivation behind this is due to the expensive evaluation that our grasp metric Q can take [20] and the fact that the convergence of the expected quality

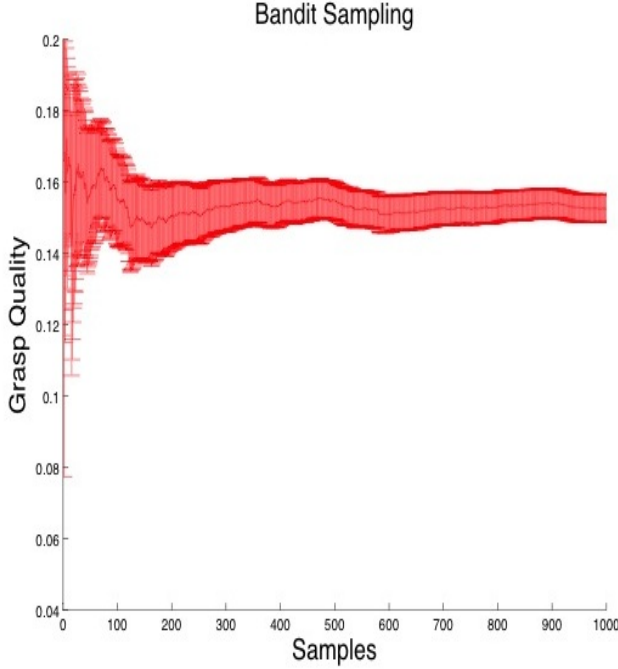of a typical grasp can take hundreds of evaluations as shown in Fig. 7.

Fig. 7: Convergence of expected grasp quality, $E(Q(g))$, for a typical grasp. You can see it can take hundreds of evaluations to correctly estimate the expected grasp quality, thus it is important to intelligently allocate sampling resources

A. Preliminaries

Compared to classical multi-arm bandit problems where the agent is evaluated on cumulative reward at each time-step, we are interested in a decoupling of the exploration and exploitation stage. The decoupling is because the agent only needs to select one grasp plan $\Gamma*$ to execute after it has sufficiently explored the other grasp plans. The agent is expected to explore the states and then at a given time, stop and choose the best grasp plan. This type of pure exploration problem with a limited amount of resources (i.e. computation time) is defined as a "budgeted multi-arm bandit problem" [16].

More formally an agent is given a set prior distributions $\mathcal{P}(1, ..., K)$ for the K arms based on the awards seen. At each interval an arm I_t is pulled based on some allocation strategy $\psi_t \in \{1, ..., K\}$. This happens until a stopping signal is given at which point an arm (or grasp plan) is chosen based on a recommendation strategy $\zeta_t \in \{1, ..., K\}$.

Performance of our polices ψ_t and ζ_t are measured according to simple regret r_t [26].

$$r_t = r(\zeta_t) = \mu^* - \mu_{\zeta_t} \tag{19}$$

$$\mu^* = \mu_j* = \max_{j=1,..,K} \mu_j \tag{20}$$

As shown in Eq. 19, simple regret is defined as the difference between the true expected value of the grasp plan your recommendation, μ_{ζ_t} and the true expected value of the best grasp plan μ^* in the set G.

B. Our Implementation

In solving Eq. 5, we want to pick the grasp plan with the highest $E(Q(\Gamma))$ determined via Monte-Carlo Integration. Due to the non-linear nature of our grasp metric, we currently do not have a way to represent the distribution on grasp quality of $p(Q(\Gamma))$. Thus, we are restricted to the type of bandit policies available to us.

In light of this we implement our allocation policy ψ_t as simple uniform allocation. This has been shown to have good performance when the number of evaluations is large [26]. We adapt pure uniform allocation by measuring the 95% confidence interval of each arm based on previous observations.If a given arm i is pulled n_i times, the confidence interval $C_{n,i}$ is defined as [14].

$$C_i = \frac{1.96\sigma_i}{\sqrt{n_i}} \tag{21}$$

An arm i is then removed from the possible options if

$$\mu_{\zeta_t} - C_{\zeta_t} > \mu_i + C_i$$

Our recommendation strategy ζ_t is to take the highest expected grasp quality at time t. In future work, we will look at using other allocation and recommendation strategies.

VII. EXPERIMENTS

For the experiments below we used common household objects shown in Fig. 2. We manually created a 25 x 25 grid, by tracing a pointcloud of the object on a table taken with a Primesense Carmine depth sensor. To accompany the SDF, we created an occupancy map, which holds 1 if the point cloud was observed and 0 if it was not observed, and a measurement noise map, which holds the variance 0-mean noise added to the SDF values. The parameters of the GPIS were selected using maximum likelihood on a held-out set of validation shapes. Our visualization technique follows the approach of [?] and consisted of drawing many shape samples from the distribution and blurring accordingly to a histogram equalization scheme.

We did experiments for the case of two hard contacts in 2-D, however our methods are not limited to this implementation. We drew random lines of actions $\gamma_1(t)$ and $\gamma_2(t)$ by sampling around a circle with radius $\sqrt{2}n$ and sampling the circles origin, then projecting onto the largest inscribing circle in the workspace.

A. Sampling from Grasps Vs. Shape

We first tested 1000 grasp plans and sampled each one 5000 times and measured the RMS error between converged expected grasp plan qualities for sampling shape Eq. 6 vs. grasps Eq. 10 was 0.004. After confirming the distributions converged close to the same value, we show the computational complexity in Fig. 8 of the two methods for evaluating 100 grasps on an $n \times n$ grid.
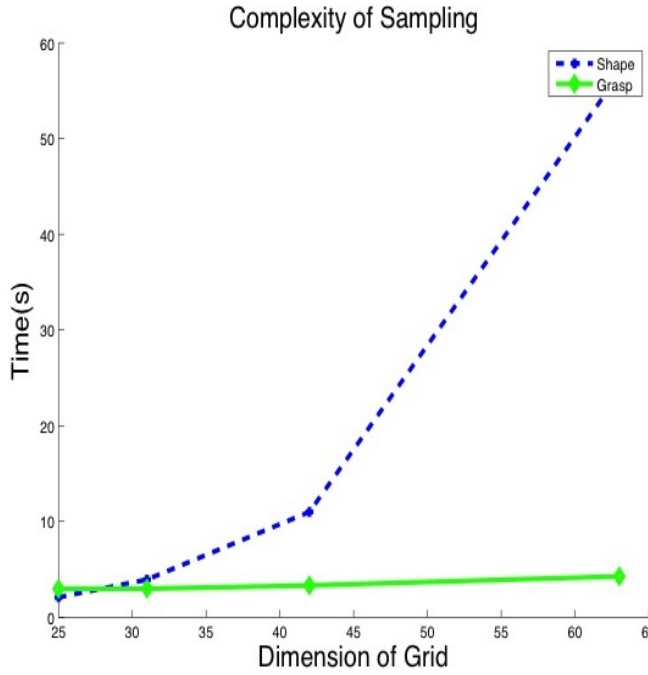
Fig. 8: Time it took to sample from 100 grasp distributions for a given resulution of the workspace. Blue line is sampling from $p(sd(\mathcal{R}))$ or shapes and Green is sampling from $p(g)$ or the calculated distribution on grasps. As you can see sampling from the calculated distributions scales much better.

B. Adaptive Sampling Technique

We consider the problem of selecting the best grasp out of a set G given a fix number of iterations I. For our experiments we look at selecting the best grasp out of a size of $|G| = 1000$ and $I = 7000$ or when the set of grasps is a single grasp. In Fig. 9, we plotted the simple regret, Eq. 19, averaged over 20 runs and compare it to the naive Monte-Carlo method that randomly chooses a grasp plan to draw a sample from . The most interesting thing is that the regret is minimized an order of magnitude faster than the naive approach, thus motivating the use of including observations as you select samples.

VIII. LIMITATIONS AND FUTURE WORK

Sampling from our distribution $p(g)$ over $p(S)$ yields a reduction in computationally complexity, but only if the number of grasps one wants to evaluate remains small relative to n^3, techniques to ensure this could be to find locally optimal potential grasps using optimization approaches [**?**].

An additional problem is that we only have an expected center of mass and not a distribution on the center of mass. This might prove to be to expensive to compute, however recent work by Panahi et al. showed a way to bound the center of mass for convex parts. Extension of his work to implicit surfaces could be of possible interest [27].

Our budgeted multi-arm bandit approach appears promising, but we still do not know how well it will perform on 3D shapes and large scale grids. Future work will be building an efficient construction of GPIS to scale to 3D. Lastly, we are interested in investigating how well our algorithm works in parallel computing to be used in the cloud computing
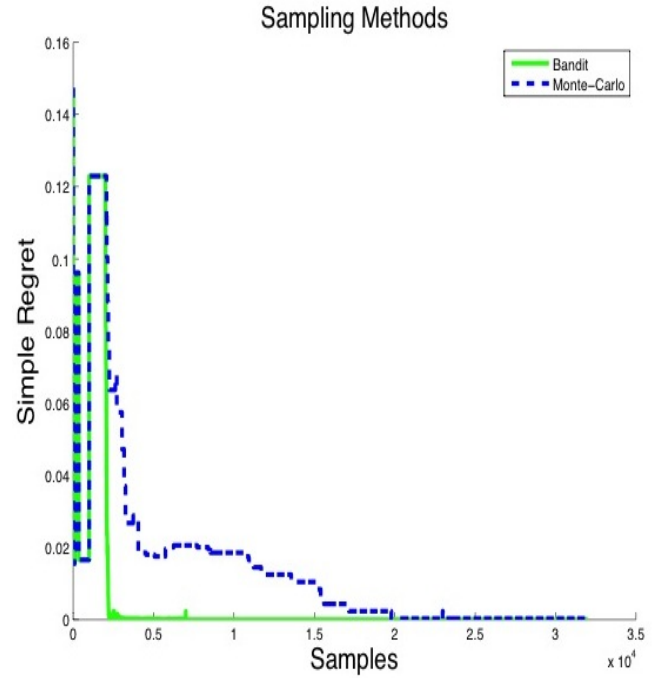

Fig. 9: Comparison of two sampling methods. Green is the adaptive bandit method that actively chooses which one to sample and Blue is the naive Monte-Carlo method. We measure their ability to converge in terms of simple regret Eq. 19 averaged over 100 runs. We had them determine the best grasp when $|G| = 1000$. As you can see our method converges much faster with an average of evaluation of 4 samples per grasp. We start the process though by deterministically evaluating every grasp 2 times to achieve a baseline, which explains the first part of the graph.

context. Furthermore, their is a large literature on formulating bandit policies and experimenting with them all will need to be done to see which one works best.

REFERENCES

[1] B. Kehoe, D. Berenson, and K. Goldberg, "Estimating part tolerance bounds based on adaptive cloud-based grasp planning with slip," in *Automation Science and Engineering (CASE), 2012 IEEE International Conference on*, pp. 1106–1113, IEEE, 2012.

[2] V. N. Christopoulos and P. Schrater, "Handling shape and contact location uncertainty in grasping two-dimensional planar objects," in *Intelligent Robots and Systems, 2007. IROS 2007. IEEE/RSJ International Conference on*, pp. 1557–1563, IEEE, 2007.

[3] Y. Zheng and W.-H. Qian, "Coping with the grasping uncertainties in force-closure analysis," *Int. J. Robotics Research (IJRR)*, vol. 24, no. 4, pp. 311–327, 2005.

[4] R. A. Newcombe, A. J. Davison, S. Izadi, P. Kohli, O. Hilliges, J. Shotton, D. Molyneaux, S. Hodges, D. Kim, and A. Fitzgibbon, "Kinectfusion: Real-time dense surface mapping and tracking," in *Mixed and augmented reality (ISMAR), 2011 10th IEEE international symposium on*, pp. 127–136, IEEE, 2011.

[5] B. Curless and M. Levoy, "A volumetric method for building complex models from range images," in *Proceedings of the 23rd annual conference on Computer graphics and interactive techniques*, pp. 303–312, ACM, 1996.

[6] S. Dragiev, M. Toussaint, and M. Gienger, "Gaussian process implicit surfaces for shape estimation and grasping," in *Proc. IEEE Int. Conf. Robotics and Automation (ICRA)*, pp. 2845–2850, 2011.

[7] G. A. Hollinger, B. Englot, F. S. Hover, U. Mitra, and G. S. Sukhatme, "Active planning for underwater inspection and the benefit of adaptivity," *Int. J. Robotics Research (IJRR)*, vol. 32, no. 1, pp. 3–18, 2013.

[8] B. Kehoe, D. Berenson, and K. Goldberg, "Toward cloud-based grasping with uncertainty in shape: Estimating lower bounds on achieving force closure with zero-slip push grasps," in *Robotics and Automation (ICRA), 2012 IEEE International Conference on*, pp. 576–583, IEEE, 2012.

[9] F. T. Pokorny and D. Kragic, "Classical grasp quality evaluation: New algorithms and theory," in *Intelligent Robots and Systems (IROS), 2013 IEEE/RSJ International Conference on*, pp. 3493–3500, IEEE, 2013.

[10] K. Y. Goldberg and M. T. Mason, "Bayesian grasping," in *Robotics and Automation, 1990. Proceedings., 1990 IEEE International Conference on*, pp. 1264–1269, IEEE, 1990.

[11] F. Stulp, E. Theodorou, J. Buchli, and S. Schaal, "Learning to grasp under uncertainty," in *Robotics and Automation (ICRA), 2011 IEEE International Conference on*, pp. 5703–5708, IEEE, 2011.

[12] J. Felip and A. Morales, "Robust sensor-based grasp primitive for a three-finger robot hand," in *Intelligent Robots and Systems, 2009. IROS 2009. IEEE/RSJ International Conference on*, pp. 1811–1816, IEEE, 2009.

[13] A. Hornung, K. M. Wurm, M. Bennewitz, C. Stachniss, and W. Burgard, "Octomap: An efficient probabilistic 3d mapping framework based on octrees," *Autonomous Robots*, vol. 34, no. 3, pp. 189–206, 2013.

[14] R. E. Caflisch, "Monte carlo and quasi-monte carlo methods," *Acta numerica*, vol. 7, pp. 1–49, 1998.

[15] A. G. Barto, *Reinforcement learning: An introduction*. MIT press, 1998.

[16] O. Madani, D. J. Lizotte, and R. Greiner, "The budgeted multi-armed bandit problem," in *Learning Theory*, pp. 643–645, Springer, 2004.

[17] C. E. Rasmussen and H. Nickisch, "Gaussian processes for machine learning (gpml) toolbox," *The Journal of Machine Learning Research*, vol. 9999, pp. 3011–3015, 2010.

[18] E. Solak, R. Murray-Smith, W. E. Leithead, D. J. Leith, and C. E. Rasmussen, "Derivative observations in gaussian process models of dynamic systems," 2003.

[19] O. Williams and A. Fitzgibbon, "Gaussian process implicit surfaces," *Gaussian Proc. in Practice*, 2007.

[20] C. Ferrari and J. Canny, "Planning optimal grasps," in *Proc. IEEE Int. Conf. Robotics and Automation (ICRA)*, pp. 2290–2295, 1992.

[21] A. T. Miller and P. K. Allen, "Graspit! a versatile simulator for robotic grasping," *Robotics & Automation Magazine, IEEE*, vol. 11, no. 4, pp. 110–122, 2004.

[22] B. León, S. Ulbrich, R. Diankov, G. Puche, M. Przybylski, A. Morales, T. Asfour, S. Moisio, J. Bohg, J. Kuffner, and R. Dillmann, *Open-GRASP: A Toolkit for Robot Grasping Simulation*, vol. 6472 of *Lecture Notes in Computer Science*, pp. 109–120. Springer Berlin / Heidelberg, 2010.

[23] N. Vahrenkamp, T. Asfour, and R. Dillmann, "Simo: A simulation and motion planning toolbo for c+,"

[24] Z. Li and S. S. Sastry, "Task-oriented optimal grasping by multifingered robot hands," *Robotics and Automation, IEEE Journal of*, vol. 4, no. 1, pp. 32–44, 1988.

[25] K. B. Petersen, "The matrix cookbook,"

[26] S. Bubeck, R. Munos, and G. Stoltz, "Pure exploration in multi-armed bandits problems," in *Algorithmic Learning Theory*, pp. 23–37, Springer, 2009.

[27] F. Panahi and A. F. van der Stappen, "Bounding the locus of the center of mass for a part with shape variation," *Computational Geometry*, vol. 47, no. 8, pp. 847–855, 2014.